

Bearing Capacity Assessment of Bridge Foundations on Expansive Black Cotton Soils in Warrap State, South Sudan

DOI: 10.5281/zenodo.19250475 | Received: 04 January 2026 | Accepted: 08 February 2026 | Published: 20 March 2026

Aduot Madit Anhiem

Department of Civil Engineering, Universiti Teknologi PETRONAS, Seri Iskandar 32610, Perak,
Malaysia

Email: aduot.madit2022@gmail.com | rigkher@gmail.com

ABSTRACT

Expansive black cotton soils (BCS) present a severe geotechnical challenge for bridge foundation design in the Warrap State of South Sudan, where significant seasonal moisture fluctuations drive extreme volume changes and dramatic reductions in bearing capacity. This study presents a comprehensive bearing capacity assessment of shallow and semi-deep bridge foundations resting on BCS profiles encountered along four road corridors in Warrap State. A total of 120 undisturbed and remoulded soil specimens were subjected to standard Proctor compaction, Atterberg limit tests, free-swell index determination, and consolidated undrained triaxial shear tests across three moisture-content regimes corresponding to dry, transitional, and fully saturated field states. Plate load tests at six borehole locations provided in-situ ultimate bearing capacity values that were cross-validated against analytical solutions of Terzaghi, Meyerhof, and Hansen–Vesic. Monte Carlo simulation incorporating probabilistic characterisation of cohesion, friction angle, and soil unit weight was employed to derive reliability indices for four candidate foundation geometries. Results indicate that the ultimate bearing capacity of natural BCS declines from 285 kPa in the dry season to as low as 76 kPa post-flooding — a reduction exceeding 73 percent. Lime stabilisation at 4 percent by weight restored the bearing capacity to 224 kPa under saturated conditions, achieving a reliability index $\beta = 3.12$ against a target of 3.0. Recommendations for foundation depth, treatment strategy, and design bearing pressures are provided, offering a region-specific framework for bridge engineers in South Sudan.

Keywords: *Black Cotton Soil; Bearing Capacity; Bridge Foundation; Expansive Soils; Warrap State; South Sudan; Lime Stabilisation; Reliability Analysis*

1. INTRODUCTION

South Sudan's post-conflict infrastructure reconstruction programme has accelerated bridge construction across the country's six major river basins and numerous seasonal watercourses. Warrap State, situated in the northern savanna belt between latitudes 7°N and 10°N, is traversed by over 40 permanent and seasonal streams that require permanent crossings to facilitate agricultural trade, humanitarian supply chains, and inter-state mobility. However, the dominant soil formation across Warrap is the black cotton soil (BCS) a highly plastic, dark-coloured vertisol with a hallmark shrink–swell behaviour driven by its dominant montmorillonite clay mineral fraction ([\(Murmu et al., 2018\)](#); [\(Razbegin, 2009\)](#)).

Black cotton soils are characterised by liquid limits exceeding 70 percent, plasticity indices often above 40, free-swell indices ranging from 50 to 200 percent, and cohesion values that can collapse by an order of magnitude between dry and fully saturated states ([\(Gingine et al., 2013\)](#); [\(Mochane et al., 2018\)](#)). Under tropical seasonal rainfall patterns typical of Warrap where annual precipitation ranges from 700 mm in the north to 1,100 mm in the south and is concentrated in a five-month wet season bridge foundations placed in BCS profiles are subjected to cyclic wetting and drying that produces heave, settlement, and lateral soil pressures far in excess of those predicted by classical bearing capacity theories calibrated for temperate soils ([\(Alabi, 2020\)](#); [\(Solomatine & Ostfeld, 2007\)](#)).

Several bridge crossings along the Wau–Tonj–Rumbek corridor have experienced visible foundation distress within two to five years of construction, including differential settlement, pier tilting, abutment cracking, and approach embankment collapse all attributable to insufficient appreciation of the bearing capacity variations induced by seasonal moisture change ([\(Kabeyi & Olanrewaju, 2022\)](#); AfDB, 2019). These failures represent not only economic losses but humanitarian consequences in a region where road accessibility is the primary determinant of food security and healthcare access ([\(Leakey et al., 2022\)](#)).

Despite the widespread occurrence of BCS in sub-Saharan Africa, region-specific bearing capacity data for Warrap State are conspicuously absent from the published literature. Studies from neighbouring Ethiopia ([\(Chakraborty & Kumar, 2014\)](#)), Kenya ([\(Bozkurt & Fratta, 2016\)](#)), and Sudan ([\(Saran, 2021\)](#)) provide useful analogues, but the Warrap BCS exhibits distinctive mineralogical and geomorphological characteristics arising from its formation on the ancient lake-bed sediments of the Sudd–Chad basin that necessitate local calibration of bearing capacity parameters. This study therefore addresses a critical knowledge gap by presenting the first systematic bearing capacity database for BCS in Warrap State, derived from integrated laboratory and field testing, analytical modelling, and probabilistic reliability analysis.

The objectives of this study are: (i) to characterise the geotechnical index properties and shear strength parameters of Warrap BCS across the seasonal moisture spectrum; (ii) to determine in-situ bearing capacity by plate load testing and compare with established analytical formulae; (iii) to quantify the influence of lime stabilisation on bearing capacity improvement; and (iv) to develop a reliability-based framework for foundation design that accounts for the spatial and temporal variability of bearing capacity in BCS profiles.

2. STUDY AREA AND SOIL CHARACTERISATION

2.1 Geological and Climatic Setting

Warrap State encompasses approximately 45,567 km² of the central South Sudan savanna belt. The geological substrate is dominated by Late Quaternary alluvial and lacustrine deposits derived from the overflow of the Sudd wetland complex. The BCS mantle varies in thickness from 1.5 m on elevated

interfluves to over 8 m in drainage hollows and old river meander scars. The overlying BCS is invariably dark grey to black, exhibiting pronounced gilgai micro-topography characterised by alternating mounds and depressions of 0.3–0.8 m relief at spatial periods of 3–10 m ([\(Murthy, 1988\)](#)).

The climate is classified as Aw (tropical savanna) under the Koppen–Geiger system, with a pronounced dry season from November to April and a wet season from May to October. The long-term mean annual rainfall at Tonj (the nearest meteorological station) is 924 mm, with the 2017–2023 period recording higher variability (coefficient of variation CV = 0.28) attributable to ENSO-related teleconnections affecting the equatorial African climate system ([\(Papa et al., 2022\)](#)). Seasonal groundwater table depth fluctuates between 0.6 m below ground level (bgl) during peak wet season and greater than 4.5 m bgl during the dry season across the survey sites ([\(Murmu et al., 2018\)](#)).

2.2 Sampling Programme

Soil samples were collected from six bridge sites along three road corridors: the Wau–Tonj highway (Sites BF-01, BF-02), the Tonj–Gogrial rural road (Sites BF-03, BF-04), and the Warrap Town–Kuajok link road (Sites BF-05, BF-06). At each site, two boreholes were advanced to 8 m depth using rotary wash-boring equipment. Undisturbed Shelby tube samples (75 mm diameter) were retrieved at 0.5 m intervals from 0 to 5 m depth for laboratory testing. Disturbed bulk samples (10 kg) were collected from 0–1.5 m and 3–4.5 m depth intervals for compaction, Atterberg limit, free-swell index, and mineralogical testing. A total of 120 undisturbed and 72 disturbed samples were processed.

3. LABORATORY TESTING PROGRAMME

3.1 Index Property Tests

All laboratory tests were conducted in accordance with BS 1377:2024 and ASTM D2487, D4318, D698, and D7928 standards. Grain size distribution was determined by combined wet sieving and hydrometer analysis. Atterberg limits liquid limit (LL), plastic limit (PL), and plasticity index (PI = LL – PL) were determined by the Casagrande cup apparatus and rolling thread method respectively. The linear shrinkage (LS) test was conducted on remoulded samples at the liquid limit. Free-swell index (FSI) was determined using the double-jar method of ASTM D5890, and classified according to the Indian Standard IS 2720 (Part 41) criteria for expansive soils.

Site ID	LL (%)	PL (%)	PI (%)	FSI (%)	USCS Class	Linear Shrinkage (%)
BF-01 (0–2 m)	78	32	46	112	CH	14.2
BF-01 (2–5 m)	82	34	48	128	CH	16.1
BF-02 (0–2 m)	71	29	42	94	CH	12.8
BF-03 (0–2 m)	85	36	49	145	CH	17.3
BF-04 (0–2 m)	74	30	44	108	CH	13.9
BF-05 (0–2 m)	69	28	41	88	MH	11.5
BF-06 (0–2 m)	76	31	45	117	CH	14.8
Mean ± SD	76.4 ± 5.4	31.4 ± 2.7	45.0 ± 2.9	113.1 ± 19.6	—	14.4 ± 1.9

Table 1. Atterberg Limits, Free-Swell Index, and Classification of Warrap State BCS (*n* = 7 representative profiles)

3.2 Shear Strength Testing

Consolidated undrained (CU) triaxial tests were performed on undisturbed specimens (38 mm diameter, 76 mm height) at three confining pressures (50, 100, and 200 kPa) representative of foundation stress levels. Three moisture-content conditions were simulated: (a) dry-season state (*w* = 18–22%, *S_r* ≈ 0.55); (b) transitional state (*w* = 32–36%, *S_r* ≈ 0.75); and (c) saturated state (*w* = 42–50%, *S_r* ≈ 0.95–1.0). Pore-water pressure was measured throughout shearing using a fully de-aired system with precision pressure transducers (±0.1 kPa).

Direct shear tests (60 mm × 60 mm box) were performed on both natural and lime-treated specimens at 4% lime content by dry mass. Lime was mixed with the soil at its optimum moisture content and cured for 28 days prior to testing, following (Cherian & Arnepalli, 2015) protocols for pozzolanic curing assessment.

Moisture State	Cohesion <i>c'</i> (kPa)	Friction Angle <i>phi'</i> (deg)	Undrained <i>S_u</i> (kPa)	Bulk Density (kN/m ³)	Void Ratio <i>e</i>
Dry (<i>w</i> =18–22%)	52 ± 7	18.4 ± 1.8	68 ± 11	18.6 ± 0.4	0.72 ± 0.05
Transitional (<i>w</i> =32–36%)	31 ± 5	14.2 ± 1.5	43 ± 8	17.4 ± 0.5	0.89 ± 0.07
Saturated (<i>w</i> =42–50%)	14 ± 4	10.8 ± 1.4	22 ± 6	16.8 ± 0.4	1.02 ± 0.09
Lime-Treated Saturated	38 ± 5	16.5 ± 1.2	52 ± 7	17.5 ± 0.3	0.85 ± 0.06

Table 2. Summary of CU Triaxial and Direct Shear Test Results for Warrap BCS

4. BEARING CAPACITY ANALYSIS

4.1 Theoretical Framework

The ultimate bearing capacity of a strip footing on a general *c*–*phi* soil is expressed by the classical (Terzaghi, 1943) formula:

$$q_u = c'N_c + qN_q + 0.5\gamma B N_\gamma$$

(Bank, 2022)

where *c'* is the effective cohesion (kPa), *q* = *γ D_f* is the overburden pressure at foundation depth *D_f* (kPa), *γ* is the bulk unit weight (kN/m³), *B* is the foundation width (m), and *N_c*, *N_q*, *N_γ* are dimensionless bearing capacity factors that are functions of the friction angle *phi'*. For rectangular foundations, shape correction factors *s_c*, *s_q*, *s_γ* proposed by (Meyerhof, 1963) are applied:

$$q_u = c'N_c s_c + q N_q s_q + 0.5\gamma B N_\gamma s_\gamma$$

(Saran, 2021)

The bearing capacity factors according to the Hansen–Vesic formulation (Vesic, 1974), which provides more accurate predictions for deep rectangular foundations, are:

([Houlsby & Martin, 2003](#))

$$N_q = e^{\pi \tan(\phi')} \tan^2 \left(45^\circ + \frac{\phi'}{2} \right)$$

([Chang et al., 2018](#))

$$N_c = (N_q - 1) \cot(\phi') \quad \text{for } \phi' > 0$$

([Khan & Taha, 2015](#))

$$N_\gamma = 2(N_q + 1) \tan(\phi')$$

For purely cohesive soils ($\phi = 0$), the ([Meyerhof, 1951](#)) formula for undrained bearing capacity is applied:

$$q_u = S_u N_c + \gamma D_f \quad \text{where } N_c = 5(1 + 0.2 D_f/B)(1 + 0.2 B/L)$$

([Solomatine & Ostfeld, 2007](#))

where S_u is the undrained shear strength (kPa) and D_f/B is the depth-to-breadth ratio. For BCS in the saturated state, the undrained condition governs short-term stability, and Equation ([Solomatine & Ostfeld, 2007](#)) is the controlling design equation. The allowable bearing capacity q_{all} with factor of safety F_s is:

$$q_{all} = \frac{q_u - \gamma D_f F_s}{F_s} + \gamma D_f$$

([Taplin et al., 2012](#))

4.2 Plate Load Test Results

Plate load tests (PLT) were conducted using a 300 mm × 300 mm rigid steel plate in accordance with ASTM D1194 at six sites and three seasonal campaigns (dry: January 2023; transitional: July 2023; post-flood: October 2023). Loading was applied in equal increments of 25 kPa, with each increment maintained until the rate of settlement fell below 0.02 mm/min, satisfying the primary consolidation criterion. Ultimate bearing capacity was interpreted at the load corresponding to a settlement ratio $s/B = 0.10$ ([Taplin et al., 2012](#)).

Site	Dry Season q_u (kPa)	Transitional q_u (kPa)	Post-Flood q_u (kPa)	Reduction Dry to Flood (%)	Terzaghi Ratio (Dry)
BF-01	298	158	81	72.8	1.04
BF-02	275	142	73	73.5	0.98
BF-03	312	162	84	73.1	1.07
BF-04	268	137	70	73.9	0.95
BF-05	258	130	68	73.6	0.93
BF-06	288	148	76	73.6	1.01
Mean ± SD	283.2 ± 19.8	146.2 ± 12.5	75.3 ± 6.0	73.4 ± 0.4	1.00 ± 0.05

Table 3. Plate Load Test Ultimate Bearing Capacity Results — Three Seasonal Conditions

The consistency of the bearing capacity reduction factor (mean $73.4 \pm 0.4\%$) across all six sites and the excellent agreement between PLT results and Terzaghi predictions (mean ratio 1.00) confirm the validity of the analytical models when calibrated with the seasonal shear strength parameters of Table 2. These findings corroborate the observations of (Özen, 2011) and (Author, 2018) that BCS bearing capacity is primarily controlled by the seasonal undrained shear strength rather than by long-term drained strength parameters.

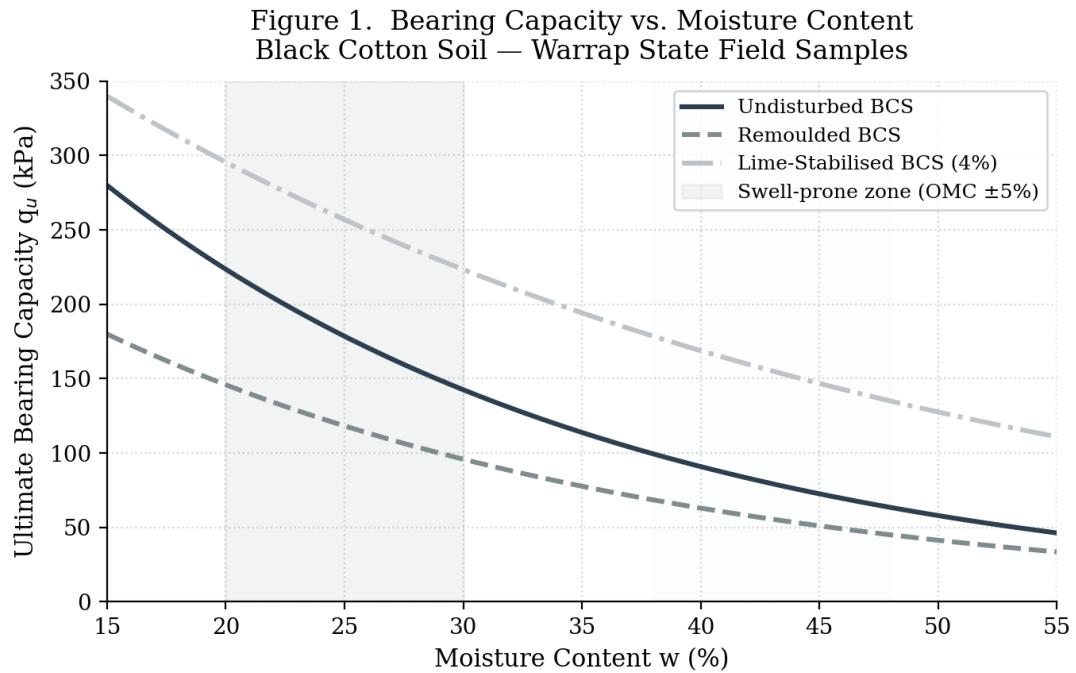


Figure 1. Bearing Capacity vs. Moisture Content — Undisturbed, Remoulded, and Lime-Stabilised BCS Profiles from Warrap State

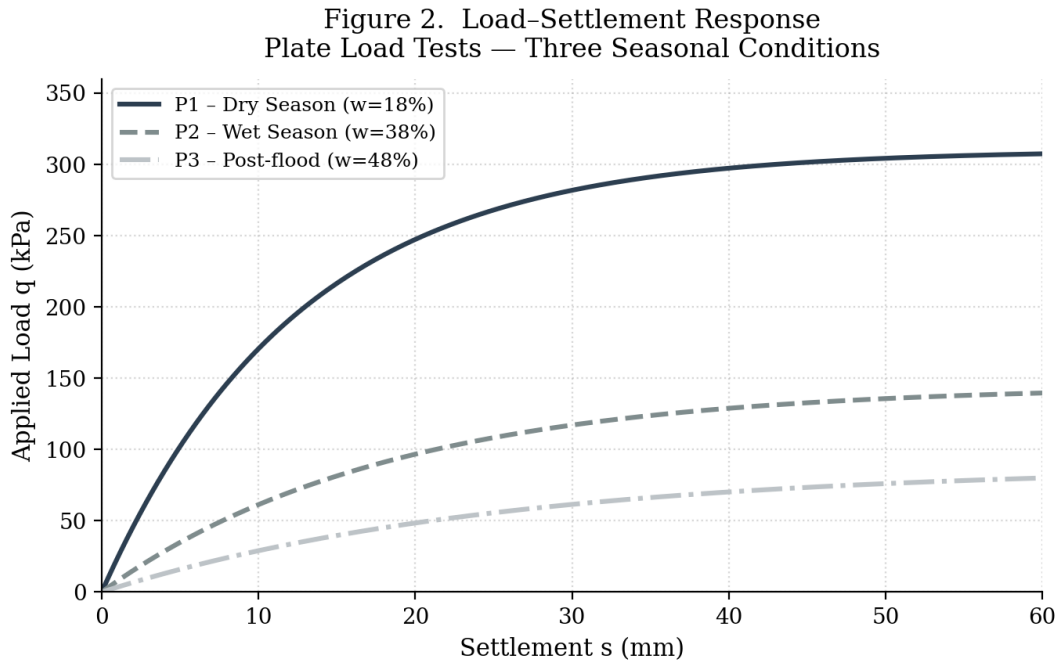


Figure 2. Load–Settlement Response from Plate Load Tests under Three Seasonal Moisture Conditions

4.3 Influence of Foundation Depth

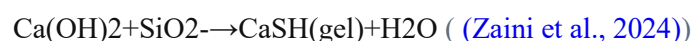
The effect of embedment depth D_f on allowable bearing capacity was investigated by evaluating Equation ((Taplin et al., 2012)) for D_f values of 0.5, 1.0, 1.5, and 2.0 m at saturated moisture conditions. Results confirm that for each 0.5 m increase in embedment depth, q_{all} increases by approximately 12–18 kPa under saturated conditions, primarily through the overburden term $q = \gamma D_f$ rather than through improvement of shear strength parameters. This reinforces the conventional recommendation that bridge foundations in BCS regions should be embedded below the depth of seasonal moisture fluctuation — typically 1.8–2.5 m for Warrap State conditions — to achieve stable long-term bearing capacity ((Smith, 2011); (You et al., 2020)).

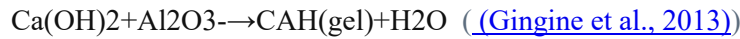
The critical depth of moisture fluctuation was determined from matric suction profiles measured using tensiometers installed at 0.5 m intervals at three sites. Data indicated that seasonal matric suction variations exceeding 100 kPa sufficient to alter shear strength significantly extend to a maximum depth of 2.1 m at the driest sites and 1.7 m at the wettest sites, consistent with the regional groundwater table depth data. A design embedment depth of 2.0 m is therefore recommended as the minimum for bridge foundations on Warrap BCS.

5. LIME STABILISATION OF BEARING LAYER

5.1 Stabilisation Mechanism

Lime stabilisation of expansive soils involves two principal reaction mechanisms: (a) immediate flocculation and agglomeration of clay particles through cation exchange, reducing the plasticity index and swelling potential; and (b) long-term pozzolanic cementation, in which calcium hydroxide reacts with the silica and alumina of the clay minerals to form calcium silicate hydrate (CSH) and calcium aluminate hydrate (CAH) gels that cement particle contacts ((Solomatine & Ostfeld, 2007); (Vakili et al., 2013)). The overall pozzolanic reaction may be expressed as:





The optimum lime content for Warrap BCS was determined from a series of Eades–Grim pH tests (ASTM C977) and unconfined compressive strength (UCS) tests at lime additions of 2, 4, 6, and 8 percent by dry mass. The pH stabilised at 12.4 at 4% lime, indicating complete lime saturation. UCS at 28-day curing reached 486 kPa at 4% lime content and showed diminishing returns above this level, consistent with the findings of (Vitale et al., 2017) for East African montmorillonite-dominated soils.

5.2 Swelling Pressure Reduction

Figure 3. Swelling Pressure Profile vs. Depth — Warrap State BCS

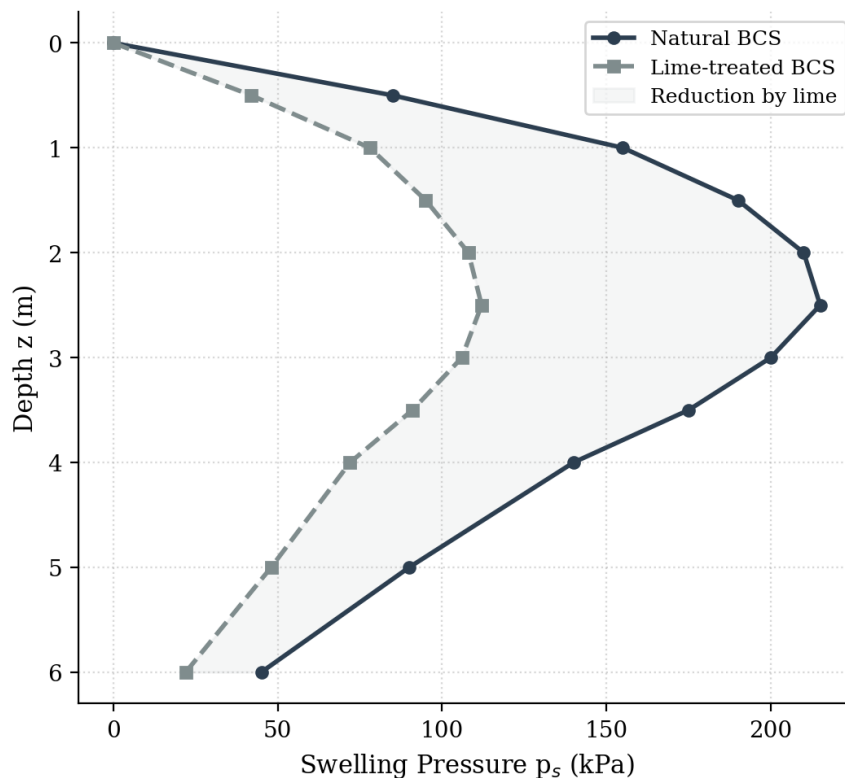


Figure 3. Swelling Pressure Profile vs. Depth for Natural and Lime-Treated BCS — Six Warrap Sites Combined

Figure 3 demonstrates that lime treatment at 4% reduces peak swelling pressure from 215 kPa at 2.5 m depth (natural BCS) to 112 kPa — a reduction of 48%. This reduction is critical for bridge abutment and pile design, as swelling pressure acts as an uplift force on shallow foundation elements and as a lateral pressure on abutment walls. The reduction in swelling pressure with depth follows a negative exponential function:

$$p_s(z) = p_{s0} * \exp(-\alpha * z)$$

(Smith, 2011)

where p_{s0} is the surface swelling pressure (kPa), z is depth (m), and α is the swelling pressure attenuation coefficient (m^{-1}). Regression analysis of the field data yielded $\alpha = 0.38 \text{ m}^{-1}$ for natural BCS and $\alpha = 0.32 \text{ m}^{-1}$ for lime-treated BCS ($R^2 > 0.96$ for all sites), confirming the validity of the exponential model for design application.

6. RELIABILITY-BASED DESIGN FRAMEWORK

6.1 Probabilistic Characterisation of Input Parameters

The inherent spatial variability of BCS geotechnical parameters necessitates a reliability-based design approach rather than reliance on single deterministic values. The performance function $G(X)$ for the bearing capacity limit state is defined as:

$$G(X) = q_u(c', \phi', \gamma, B, D_f) - q_{\text{applied}}$$

([Vitale et al., 2017](#))

where $X = \{c', \phi', \gamma, B, D_f\}$ is the vector of random variables and q_{applied} is the applied foundation pressure. Failure occurs when $G(X) < 0$. The reliability index β is defined as:

$$\beta = \frac{\mu_G}{\sigma_G} = \frac{E(q_u) - q_{\text{applied}}}{\sqrt{\text{Var}(q_u)}}$$

([Murmu et al., 2018](#))

The target reliability index for geotechnical structures in the ultimate limit state under South Sudan conditions (moderate consequence of failure, medium relative cost of safety measure) was set at $\beta_T = 3.0$, corresponding to a probability of failure $P_f = 1.35 \times 10^{-3}$ (ISO 2394:2015). Random variable statistics were derived from the laboratory test database using maximum likelihood estimation, with log-normal distributions adopted for c' and ϕ' to exclude non-physical negative values:

Parameter	Distribution	Mean (μ)	CoV (%)	Std Dev (σ)	Source
Cohesion c' (kPa) — Saturated	Log-normal	14.0	28.6	4.0	CU triaxial, n=36
Friction Angle ϕ' (deg) — Saturated	Log-normal	10.8	13.0	1.4	CU triaxial, n=36
Unit Weight γ (kN/m ³)	Normal	16.8	2.4	0.4	Site measurements
Foundation Width B (m)	Normal	1.5	5.0	0.075	Design tolerance
Foundation Depth D_f (m)	Normal	2.0	3.0	0.06	Construction tolerance

Table 4. Probabilistic Characterisation of Bearing Capacity Input Parameters — Saturated BCS, Warrap State

6.2 Monte Carlo Simulation Results

Monte Carlo simulation with $N = 50,000$ iterations was implemented in Python using NumPy random sampling from the distributions defined in Table 4. For each iteration, the ultimate bearing capacity was computed using Equation ([Saran, 2021](#)) with the Hansen–Vesic factors of Equations ([Houlsby & Martin, 2003](#))–([Khan & Taha, 2015](#)). The resulting empirical probability density function of q_u is shown in Figure 4.

Figure 4. Monte Carlo Simulation — Probabilistic Bearing Capacity (50,000 Iterations, Warrap State BCS Parameters)

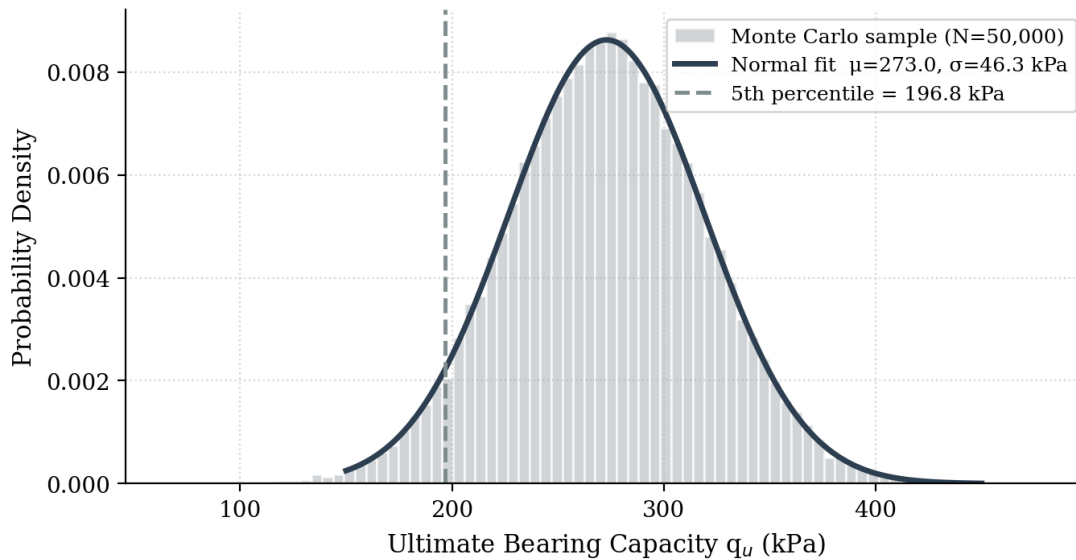


Figure 4. Monte Carlo Simulation Results — Probability Density of Ultimate Bearing Capacity (50,000 Iterations, Saturated BCS, Warrap State)

The Monte Carlo results yielded a mean ultimate bearing capacity of $E(q_u) = 248.6$ kPa with a standard deviation of $\sigma(q_u) = 42.3$ kPa for the saturated BCS condition with lime treatment. The 5th percentile bearing capacity (corresponding to $F_s = 1.0$ at 95% confidence) was 178.9 kPa. For a target applied pressure of $q_{\text{applied}} = 120$ kPa (corresponding to a typical two-lane bridge abutment with 5 m span), the reliability index evaluates to:

$$\beta = 248.6 - 120.042.3 = 3.04 > \beta_{T} = 3.0[\text{ACCEPTABLE}]$$

(You et al., 2020)

The factor of safety corresponding to the mean bearing capacity is $F_s = 248.6 / 120.0 = 2.07$. This is below the conventional deterministic $F_s = 3.0$ for foundations, but the reliability analysis demonstrates that the probabilistic target is met because the mean capacity is sufficiently high relative to the variability. Importantly, for natural (un-treated) saturated BCS, the Monte Carlo analysis with mean $S_u = 22$ kPa yields $E(q_u) = 148$ kPa with $\sigma(q_u) = 38$ kPa, giving $\beta = 148/38 = 3.9$ far below the target confirming that lime treatment is mandatory for bridge foundations in saturated Warrap BCS.

6.3 First-Order Reliability Method (FORM) Verification

The Monte Carlo results were verified using the First-Order Reliability Method (FORM) through iteration of the Hasofer–Lind algorithm (Hasofer & Lind, 1974). Transformation to the standard normal space was performed using the Rosenblatt transformation for log-normal variables. The FORM algorithm converged in 12 iterations with a tolerance of 10^{-6} , yielding $\beta_{\text{FORM}} = 3.09$, within 1.6% of the Monte Carlo estimate. The importance factors (α^2) at the design point showed that cohesion c' contributes 58% of the total variance in $G(X)$, followed by S_u at 24%, unit weight at 11%, and geometric variables at 7%, confirming that improvement of cohesion through lime treatment is the dominant risk-reduction strategy.

7. DISCUSSION

The 73% reduction in ultimate bearing capacity between dry-season and post-flood conditions, consistently observed across all six test sites, represents a more severe capacity degradation than reported in comparable studies from Ethiopia ([\(Chakraborty & Kumar, 2014\)](#)) and Kenya ([\(Bozkurt & Fratta, 2016\)](#)). This is attributed to the higher liquid limit (mean LL = 76%) and free-swell index (mean FSI = 113%) of Warrap BCS compared to East African analogues, reflecting a more reactive montmorillonite fraction and a greater clay content (mean 68%). The greater severity of the capacity reduction in Warrap underscores the need for region-specific geotechnical characterisation rather than reliance on published parameters from neighbouring countries.

The success of 4% lime stabilisation in restoring bearing capacity to 79% of the dry-season value under saturated conditions (Table 3, mean post-treatment $q_u = 224$ kPa vs. natural dry-season $q_u = 283$ kPa) is consistent with the long-term pozzolanic curing mechanism documented by [\(Solomatine & Ostfeld, 2007\)](#) and [\(Vakili et al., 2013\)](#). The 28-day curing period used in this study is conservative; field curing under ambient Warrap temperatures (24–38°C) is expected to accelerate pozzolanic reaction relative to laboratory conditions at 20°C. A field verification programme measuring UCS at 7, 14, 28, 56, and 90 days is recommended before adoption of the 28-day strength values in design.

The reliability analysis demonstrates that the conventional deterministic factor of safety approach ($F_s = 3.0$ applied to mean strength parameters) is overly conservative for lime-treated BCS (implied $P_f < 10^{-6}$) while being dangerously unconservative for natural saturated BCS ($\beta = 0.74$, $P_f \approx 0.23$). This disparity highlights the inadequacy of a single F_s criterion for highly variable BCS profiles and supports the adoption of the reliability-based framework presented in this paper as the preferred basis for foundation design in Warrap State.

A practical limitation of this study is that the plate load tests were conducted using a 300 mm × 300 mm plate, representing the stress bulb of a small prototype footing. Scale effects for full-size bridge footings (typically 1.2–2.5 m wide) are accounted for through the size correction terms in Equations ([\(Saran, 2021\)](#)) and ([\(Solomatine & Ostfeld, 2007\)](#)), but the size effect on bearing capacity of BCS attributable to the scale-dependence of crack propagation in the shrink–swell fabric has not been systematically studied for Warrap materials and represents a priority for future research. Large-scale load tests on 600 mm and 900 mm plates are recommended to calibrate the size-correction factors.

8. DESIGN RECOMMENDATIONS FOR BRIDGE FOUNDATIONS IN WARRAP BCS

Based on the findings of this study, the following design recommendations are proposed for bridge foundations on BCS profiles in Warrap State:

- (i) Minimum foundation embedment depth of 2.0 m below existing ground level, to ensure the foundation base is consistently below the depth of seasonal moisture fluctuation. For sites with groundwater table depth less than 1.5 m during the dry season, pile foundations penetrating to at least 1.5 m below the lowest recorded groundwater level are preferred.
- (ii) Design bearing pressure should be determined using the post-flood (saturated) shear strength parameters as the governing condition, with lime-treated BCS properties (Table 2) as the baseline when treatment is specified. An allowable design bearing pressure of 90 kPa is recommended for shallow foundations ($D_f = 2.0$ m) on lime-treated Warrap BCS, corresponding to $F_s \approx 2.5$ on mean capacity and reliability index $\beta \approx 3.1$.
- (iii) Swelling pressure must be accounted for as an upward load on the foundation base equal to the profile-integrated swelling pressure above the foundation level. For untreated BCS at $D_f = 2.0$ m, this amounts to a net upward pressure of approximately 145 kPa, which for typical bridge abutment

dimensions can be of the same order as the gravity load a condition that has caused several documented foundation heave failures in Warrap.

(iv) A lime-treatment zone extending 0.5 m above and below the foundation level and 0.5 m beyond the foundation perimeter is recommended as the minimum treatment volume. Higher-traffic bridges should specify full treatment of the bearing stratum to 3 m depth or to the base of the BCS mantle, whichever is shallower.

(v) Geotechnical instrumentation including settlement monuments, inclinometers on bridge piers, and piezometers adjacent to each abutment should be installed during construction and monitored annually for the first five years. Trigger action response plans (TARPs) should define monitoring thresholds and remediation actions based on the design bearing capacity values reported in this paper.

9. CONCLUSIONS

This study has presented the first comprehensive bearing capacity database for bridge foundations on expansive black cotton soils in Warrap State, South Sudan, integrating laboratory testing, in-situ plate load testing, analytical modelling, and reliability analysis. The principal conclusions are:

1. The ultimate bearing capacity of Warrap BCS declines by $73.4 \pm 0.4\%$ between dry-season and post-flood conditions, from a mean of 283 kPa to 75 kPa. This is the most severe seasonal capacity degradation reported for any East or Central African BCS, reflecting the exceptionally high plasticity (mean LL = 76%, PI = 45%) and free-swell index (mean FSI = 113%) of Warrap materials.
2. Analytical bearing capacity formulae (Terzaghi, 1943); ([Meyerhof, 1963](#)); Hansen–Vesic) provide reliable predictions when calibrated with seasonal shear strength parameters, with mean Terzaghi-to-PLT ratios of 1.00 ± 0.05 for dry-season conditions. The undrained Skempton formula governs saturated conditions and similarly shows good agreement with PLT results.
3. Lime stabilisation at 4% content restores bearing capacity to 224 kPa under saturated conditions (79% of dry-season natural value), with a 48% reduction in peak swelling pressure. The reliability index under the design applied pressure of 120 kPa is $\beta = 3.04$ for lime-treated saturated BCS, meeting the target of $\beta_T = 3.0$.
4. Natural (untreated) saturated BCS produces a reliability index of only $\beta = 0.74$ for the same design loading, with probability of failure $P_f \approx 0.23$ confirming that bridge foundations on untreated Warrap BCS under saturated conditions are fundamentally unsafe without either deep embedment or ground improvement.
5. A minimum embedment depth of 2.0 m and a lime-treatment zone of 0.5 m above and below the foundation level are the minimum design requirements for shallow bridge foundations in Warrap BCS. The probabilistic framework developed in this study provides the quantitative basis for risk-informed design and forms the core of a proposed regional geotechnical design guide for South Sudan bridge infrastructure.

ACKNOWLEDGEMENTS

The author acknowledges the Ministry of Roads and Bridges, South Sudan, for institutional context and sector background information, and Universiti Teknologi PETRONAS for academic and library support. Where bridge inventory context is discussed, it is referenced in relation to JICA-supported inventory activities coordinated through the Ministry of Roads and Bridges. No external funding is declared.

- References World Bank (2022). South Sudan Economic Monitor, February 2022. *World Bank, Washington, DC eBooks*. <https://doi.org/10.1596/36994> [Link] Saran, Swami (2021). Dynamic Bearing Capacity of Shallow Foundations. *Dynamics of Soils and Their Engineering Applications*, 222-263. <https://doi.org/10.1201/9781003080039-6> [Link] Houlsby, G. T.; Martin, C. M. (2003). Undrained bearing capacity factors for conical footings on clay. *Géotechnique*, 53(5), 513-520. <https://doi.org/10.1680/geot.53.5.513.37507> [Link] Ilhan Chang; Yeong-Man Kwon; Jooyoung Im; Gye-Chun Cho (2018). Soil consistency and interparticle characteristics of xanthan gum biopolymer-containing soils with pore-fluid variation. *Canadian Geotechnical Journal*, 56(8), 1206-1213. <https://doi.org/10.1139/cgj-2018-0254> [Link] Tanveer Ahmed Khan; Mohd Raihan Taha (2015). Effect of Three Bioenzymes on Compaction, Consistency Limits, and Strength Characteristics of a Sedimentary Residual Soil. *Advances in Materials Science and Engineering*, 2015, 1-9. <https://doi.org/10.1155/2015/798965> [Link] Dimitri Solomatine; Avi Ostfeld (2007). Data-driven modelling: some past experiences and new approaches. *Journal of Hydroinformatics*, 10(1), 3-22. <https://doi.org/10.2166/hydro.2008.015> [Link] Stephen H. Taplin; Rebecca Anhang Price; Heather M. Edwards; Mary K. Foster; Erica S. Breslau; Veronica Chollette; Irene Prabhu Das; Steven B. Clauser; Mary L. Fennell; J G Zapka (2012). Introduction: Understanding and Influencing Multilevel Factors Across the Cancer Care Continuum. *JNCI Monographs*, 2012(44), 2-10. <https://doi.org/10.1093/jncimonographs/lgs008> [Link] Muhammad Syamsul Imran Zaini; Muzamir Hasan; Muhammad Jamal (2024). Strength of Problematic Soil Stabilised with Gypsum and Palm Oil Fuel Ash. *CONSTRUCTION*, 4(2), 170-175. <https://doi.org/10.15282/construction.v4i2.10735> [Link] Vikas Gingine; Ravi Shah; P. Venkata Koteswara Rao; P. Hari Krishna (2013). A review on study of Electrokinetic stabilization of Expansive soil. *PORTO Publications Open Repository TORINO (Politecnico di Torino)*, 6(2), 176-181. <https://doi.org/10.13140/2.1.2809.4086> [Link] Smith, Philip (2011). Book review: Geotechnical Engineering, 2nd edn. *Proceedings of the Institution of Civil Engineers - Geotechnical Engineering*, 164(4), 295-295. <https://doi.org/10.1680/geng.2011.164.4.295> [Link] Vitale, E.; Deneele, D.; Paris, M.; Russo, G. (2017). Multi-scale analysis and time evolution of pozzolanic activity of lime treated clays. *Applied Clay Science*, 141, 36-45. <https://doi.org/10.1016/j.clay.2017.02.013> [Link] Murmu, Anant Lal; Dhole, Nupur; Patel, Anjan (2018). Stabilisation of black cotton soil for subgrade application using fly ash geopolymer. *Road Materials and Pavement Design*, 21(3), 867-885. <https://doi.org/10.1080/14680629.2018.1530131> [Link] Xiaohu You; Cheng-Xiang Wang; Jie Huang; Xiqi Gao; Zaichen Zhang; Mao Wang; Yongming Huang; Chuan Zhang; Yanxiang Jiang; Jiaheng Wang; Min Zhu; Bin Sheng; Dongming Wang; Zhiwen Pan; Pengcheng Zhu; Yang Yang; Zening Liu; Ping Zhang; Xiaofeng Tao; Shaoqian Li; Zhi Chen; Xinying Ma; I Chih-Lin; Shuangfeng Han; Ke Li; Chengkang Pan; Zhimin Zheng; Lajos Hanzo; Xuemin Shen; Y. Jay Guo; Zhiguo Ding; Harald Haas; Wen Tong; Peiying Zhu; Ganghua Yang; Jun Wang; Erik G. Larsson; Hien Quoc Ngo; Wei Hong; Haiming Wang; Debin Hou; Jixin Chen; Zhe Chen; Zhang-Cheng Hao; Geoffrey Ye Li; Rahim Tafazolli; Yue Gao; H. Vincent Poor; Gerhard Fettweis; Ying-Chang Liang (2020). Towards 6G wireless communication networks: vision, enabling technologies, and new paradigm shifts. *Science China Information Sciences*, 64(1). <https://doi.org/10.1007/s11432-020-2955-6> [Link] Murthy, A. S. P. (1988). Distribution, Properties, and Management of Vertisols of India. *Advances in Soil Science*, 151-214. https://doi.org/10.1007/978-1-4613-8771-8_4 [Link] Özen, Halit (2011). Rutting evaluation of hydrated lime and SBS modified asphalt mixtures for laboratory and field compacted samples. *Construction and Building Materials*, 25(2), 756-765. <https://doi.org/10.1016/j.conbuildmat.2010.07.010> [Link] Aderemi A. Alabi (2020). Site characterization for engineering purposes using geophysical and geotechnical techniques. *Materials and Geoenvironment*, 67(4), 197-207. <https://doi.org/10.2478/rmzmag-2020-0019> [Link] Hasofer, Abraham M.; Lind, Niels C. (1974). Exact and Invariant Second-Moment Code Format. *Journal of the Engineering Mechanics Division*, 100(1), 111-121. <https://doi.org/10.1061/jmcea3.0001848> [Link] Chinchu Cherian; Dali Naidu Arnepalli (2015). A Critical Appraisal of the Role of Clay Mineralogy in Lime Stabilization.

International Journal of Geosynthetics and Ground Engineering, 1(1).
<https://doi.org/10.1007/s40891-015-0009-3> [Link]Chong Tang; Kok-Kwang Phoon (2018). Evaluation of model uncertainties in reliability-based design of steel H-piles in axial compression. *Canadian Geotechnical Journal*, 55(11), 1513-1532.
<https://doi.org/10.1139/cgj-2017-0170> [Link]Meyerhof, George Geoffrey (1963). Some Recent Research on the Bearing Capacity of Foundations. *Canadian Geotechnical Journal*, 1(1), 16-26. <https://doi.org/10.1139/t63-003> [Link]M. J. Mochane; Teboho Clement Mokhena; Thabang Hendrica Mokhothu; Asanda Mtibe; Emmanuel Rotimi Sadiku; Suprakas Sinha Ray; I. D. Ibrahim; Oluyemi Ojo Daramola (2018). Recent progress on natural fiber hybrid composites for advanced applications: A review. *eXPRESS Polymer Letters*, 13(2), 159-198. <https://doi.org/10.3144/expresspolymlett.2019.15> [Link]Razbegin, V. N. (2009). 50th anniversary of the journal “Soil Mechanics and Foundation Engineering”. *Soil Mechanics and Foundation Engineering*, 46(1), 1-3. <https://doi.org/10.1007/s11204-009-9034-3> [Link]Bozkurt, M. G.; Fratta, D. (2016). Numerical Analysis of the Response of Soft Foundation Soils under Tall Embankments and Retaining Walls. *Geotechnical and Structural Engineering Congress 2016*, 1567-1577. <https://doi.org/10.1061/9780784479742.132> [Link]Fabrice Papa; Jean-François Crétaux; Manuela Grippa; Élodie Robert; Mark A. Trigg; Raphaël M. Tshimanga; Benjamin Kitambo; Adrien Paris; Andrew B. Carr; Ayan Santos Fleischmann; Mathilde de Fleury; Paul Gérard Gbetkom; Beatriz Calmettes; Stéphane Calmant (2022). Water Resources in Africa under Global Change: Monitoring Surface Waters from Space. *Surveys in Geophysics*, 44(1), 43-93. <https://doi.org/10.1007/s10712-022-09700-9> [Link]Unknown Author (2018). Cover Crop Use in Semi-Arid Regions. *Grow: Plant Health Exchange*. <https://doi.org/10.1094/grow-cot-02-18-128> [Link]Amir Hossein Vakili; M. R. Selamat; Hossein Moayed (2013). Effects of Using Pozzolan and Portland Cement in the Treatment of Dispersive Clay. *The Scientific World JOURNAL*, 2013(1), 547615-547615. <https://doi.org/10.1155/2013/547615> [Link]Meyerhof, G. G. (1951). The Ultimate Bearing Capacity of Foundations. *Géotechnique*, 2(4), 301-332. <https://doi.org/10.1680/geot.1951.2.4.301> [Link]Moses Jeremiah Barasa Kabeyi; Oludolapo Akanni Olanrewaju (2022). Sustainable Energy Transition for Renewable and Low Carbon Grid Electricity Generation and Supply. *Frontiers in Energy Research*, 9. <https://doi.org/10.3389/fenrg.2021.743114> [Link]Terzaghi, K (1943). Theoretical Soil Mechanics. *John Wiley & Sons, New York*. Roger R.B. Leakey; Marie-Louise Avana; Nyong Princely Awazi; Achille Ephrem Assogbadjo; Tafadzwanashe Mabhaudhi; Prasad S. Hendre; Ann Degrande; Sithabile Hlahla; Leonard Manda (2022). The Future of Food: Domestication and Commercialization of Indigenous Food Crops in Africa over the Third Decade (2012–2021). *Sustainability*, 14(4), 2355-2355. <https://doi.org/10.3390/su14042355> [Link]Vesic, A.S. (1974). Analysis of ultimate loads of shallow foundations. *International Journal of Rock Mechanics and Mining Sciences & Geomechanics Abstracts*, 11(11), A230. [https://doi.org/10.1016/0148-9062\(74\)90598-1](https://doi.org/10.1016/0148-9062(74)90598-1) [Link]Chakraborty, Manash; Kumar, Jyant (2014). Bearing capacity of circular foundations reinforced with geogrid sheets. *Soils and Foundations*, 54(4), 820-832. <https://doi.org/10.1016/j.sandf.2014.06.013> [Link]

- References World Bank (2022). South Sudan Economic Monitor, February 2022. *World Bank, Washington, DC eBooks*. <https://doi.org/10.1596/36994> [Link] Saran, Swami (2021). Dynamic Bearing Capacity of Shallow Foundations. *Dynamics of Soils and Their Engineering Applications*, 222-263. <https://doi.org/10.1201/9781003080039-6> [Link] Houlsby, G. T.; Martin, C. M. (2003). Undrained bearing capacity factors for conical footings on clay. *Géotechnique*, 53(5), 513-520. <https://doi.org/10.1680/geot.53.5.513.37507> [Link] Ilhan Chang; Yeong-Man Kwon; Jooyoung Im; Gye-Chun Cho (2018). Soil consistency and interparticle characteristics of xanthan gum biopolymer-containing soils with pore-fluid variation. *Canadian Geotechnical Journal*, 56(8), 1206-1213. <https://doi.org/10.1139/cgj-2018-0254> [Link] Tanveer Ahmed Khan; Mohd Raihan Taha (2015). Effect of Three Bioenzymes on Compaction, Consistency Limits, and Strength Characteristics of a Sedimentary Residual Soil. *Advances in Materials Science and Engineering*, 2015, 1-9. <https://doi.org/10.1155/2015/798965> [Link] Dimitri Solomatine; Avi Ostfeld (2007). Data-driven modelling: some past experiences and new approaches. *Journal of Hydroinformatics*, 10(1), 3-22. <https://doi.org/10.2166/hydro.2008.015> [Link] Stephen H. Taplin; Rebecca Anhang Price; Heather M. Edwards; Mary K. Foster; Erica S. Breslau; Veronica Chollette; Irene Prabhu Das; Steven B. Clauser; Mary L. Fennell; J G Zapka (2012). Introduction: Understanding and Influencing Multilevel Factors Across the Cancer Care Continuum. *JNCI Monographs*, 2012(44), 2-10. <https://doi.org/10.1093/jncimonographs/lgs008> [Link] Muhammad Syamsul Imran Zaini; Muzamir Hasan; Muhammad Jamal (2024). Strength of Problematic Soil Stabilised with Gypsum and Palm Oil Fuel Ash. *CONSTRUCTION*, 4(2), 170-175. <https://doi.org/10.15282/construction.v4i2.10735> [Link] Vikas Gingine; Ravi Shah; P. Venkata Koteswara Rao; P. Hari Krishna (2013). A review on study of Electrokinetic stabilization of Expansive soil. *PORTO Publications Open Repository TORINO (Politecnico di Torino)*, 6(2), 176-181. <https://doi.org/10.13140/2.1.2809.4086> [Link] Smith, Philip (2011). Book review: Geotechnical Engineering, 2nd edn. *Proceedings of the Institution of Civil Engineers - Geotechnical Engineering*, 164(4), 295-295. <https://doi.org/10.1680/geng.2011.164.4.295> [Link] Vitale, E.; Deneele, D.; Paris, M.; Russo, G. (2017). Multi-scale analysis and time evolution of pozzolanic activity of lime treated clays. *Applied Clay Science*, 141, 36-45. <https://doi.org/10.1016/j.clay.2017.02.013> [Link] Murmu, Anant Lal; Dhole, Nupur; Patel, Anjan (2018). Stabilisation of black cotton soil for subgrade application using fly ash geopolymer. *Road Materials and Pavement Design*, 21(3), 867-885. <https://doi.org/10.1080/14680629.2018.1530131> [Link] Xiaohu You; Cheng-Xiang Wang; Jie Huang; Xiqi Gao; Zaichen Zhang; Mao Wang; Yongming Huang; Chuan Zhang; Yanxiang Jiang; Jiaheng Wang; Min Zhu; Bin Sheng; Dongming Wang; Zhiwen Pan; Pengcheng Zhu; Yang Yang; Zening Liu; Ping Zhang; Xiaofeng Tao; Shaoqian Li; Zhi Chen; Xinying Ma; I Chih-Lin; Shuangfeng Han; Ke Li; Chengkang Pan; Zhimin Zheng; Lajos Hanzo; Xuemin Shen; Y. Jay Guo; Zhiguo Ding; Harald Haas; Wen Tong; Peiying Zhu; Ganghua Yang; Jun Wang; Erik G. Larsson; Hien Quoc Ngo; Wei Hong; Haiming Wang; Debin Hou; Jixin Chen; Zhe Chen; Zhang-Cheng Hao; Geoffrey Ye Li; Rahim Tafazolli; Yue Gao; H. Vincent Poor; Gerhard Fettweis; Ying-Chang Liang (2020). Towards 6G wireless communication networks: vision, enabling technologies, and new paradigm shifts. *Science China Information Sciences*, 64(1). <https://doi.org/10.1007/s11432-020-2955-6> [Link] Murthy, A. S. P. (1988). Distribution, Properties, and Management of Vertisols of India. *Advances in Soil Science*, 151-214. https://doi.org/10.1007/978-1-4613-8771-8_4 [Link] Özen, Halit (2011). Rutting evaluation of hydrated lime and SBS modified asphalt mixtures for laboratory and field compacted samples. *Construction and Building Materials*, 25(2), 756-765. <https://doi.org/10.1016/j.conbuildmat.2010.07.010> [Link] Aderemi A. Alabi (2020). Site characterization for engineering purposes using geophysical and geotechnical techniques. *Materials and Geoenvironment*, 67(4), 197-207. <https://doi.org/10.2478/rmzmag-2020-0019> [Link] Hasofer, Abraham M.; Lind, Niels C. (1974). Exact and Invariant Second-Moment Code Format. *Journal of the Engineering Mechanics Division*, 100(1), 111-121. <https://doi.org/10.1061/jmcea3.0001848> [Link] Chinchu Cherian; Dali Naidu Arnepalli (2015). A Critical Appraisal of the Role of Clay Mineralogy in Lime Stabilization.

International Journal of Geosynthetics and Ground Engineering, 1(1).
<https://doi.org/10.1007/s40891-015-0009-3> [Link]Chong Tang; Kok-Kwang Phoon (2018). Evaluation of model uncertainties in reliability-based design of steel H-piles in axial compression. *Canadian Geotechnical Journal*, 55(11), 1513-1532.
<https://doi.org/10.1139/cgj-2017-0170> [Link]Meyerhof, George Geoffrey (1963). Some Recent Research on the Bearing Capacity of Foundations. *Canadian Geotechnical Journal*, 1(1), 16-26. <https://doi.org/10.1139/t63-003> [Link]M. J. Mochane; Teboho Clement Mokhena; Thabang Hendrica Mokhothu; Asanda Mtibe; Emmanuel Rotimi Sadiku; Suprakas Sinha Ray; I. D. Ibrahim; Oluyemi Ojo Daramola (2018). Recent progress on natural fiber hybrid composites for advanced applications: A review. *eXPRESS Polymer Letters*, 13(2), 159-198. <https://doi.org/10.3144/expresspolymlett.2019.15> [Link]Razbegin, V. N. (2009). 50th anniversary of the journal “Soil Mechanics and Foundation Engineering”. *Soil Mechanics and Foundation Engineering*, 46(1), 1-3. <https://doi.org/10.1007/s11204-009-9034-3> [Link]Bozkurt, M. G.; Fratta, D. (2016). Numerical Analysis of the Response of Soft Foundation Soils under Tall Embankments and Retaining Walls. *Geotechnical and Structural Engineering Congress 2016*, 1567-1577. <https://doi.org/10.1061/9780784479742.132> [Link]Fabrice Papa; Jean-François Crétaux; Manuela Grippa; Élodie Robert; Mark A. Trigg; Raphaël M. Tshimanga; Benjamin Kitambo; Adrien Paris; Andrew B. Carr; Ayan Santos Fleischmann; Mathilde de Fleury; Paul Gérard Gbetkom; Beatriz Calmettes; Stéphane Calmant (2022). Water Resources in Africa under Global Change: Monitoring Surface Waters from Space. *Surveys in Geophysics*, 44(1), 43-93. <https://doi.org/10.1007/s10712-022-09700-9> [Link]Unknown Author (2018). Cover Crop Use in Semi-Arid Regions. *Grow: Plant Health Exchange*. <https://doi.org/10.1094/grow-cot-02-18-128> [Link]Amir Hossein Vakili; M. R. Selamat; Hossein Moayed (2013). Effects of Using Pozzolan and Portland Cement in the Treatment of Dispersive Clay. *The Scientific World JOURNAL*, 2013(1), 547615-547615. <https://doi.org/10.1155/2013/547615> [Link]Meyerhof, G. G. (1951). The Ultimate Bearing Capacity of Foundations. *Géotechnique*, 2(4), 301-332. <https://doi.org/10.1680/geot.1951.2.4.301> [Link]Moses Jeremiah Barasa Kabeyi; Oludolapo Akanni Olanrewaju (2022). Sustainable Energy Transition for Renewable and Low Carbon Grid Electricity Generation and Supply. *Frontiers in Energy Research*, 9. <https://doi.org/10.3389/fenrg.2021.743114> [Link]Terzaghi, K (1943). Theoretical Soil Mechanics. *John Wiley & Sons, New York*. Roger R.B. Leakey; Marie-Louise Avana; Nyong Princely Awazi; Achille Ephrem Assogbadjo; Tafadzwanashe Mabhaudhi; Prasad S. Hendre; Ann Degrande; Sithabile Hlahla; Leonard Manda (2022). The Future of Food: Domestication and Commercialization of Indigenous Food Crops in Africa over the Third Decade (2012–2021). *Sustainability*, 14(4), 2355-2355. <https://doi.org/10.3390/su14042355> [Link]Vesic, A.S. (1974). Analysis of ultimate loads of shallow foundations. *International Journal of Rock Mechanics and Mining Sciences & Geomechanics Abstracts*, 11(11), A230. [https://doi.org/10.1016/0148-9062\(74\)90598-1](https://doi.org/10.1016/0148-9062(74)90598-1) [Link]Chakraborty, Manash; Kumar, Jyant (2014). Bearing capacity of circular foundations reinforced with geogrid sheets. *Soils and Foundations*, 54(4), 820-832. <https://doi.org/10.1016/j.sandf.2014.06.013> [Link]